Dynamical attractors in early Universe models: Bounce and Genesis scenarios

Based on arXiv:2610.36036

Yulia Ageeva[1,2,3] **Andrey Sharofeev**[1,3]

[1]INR RAS
[2]ITMP
[3]MSU

The 8th International Conference on Particle Physics and Astrophysics
October 29, 2026

Why study cosmological attractors?

Forward evolution: do nearby homogeneous histories converge?

Inverse reconstruction: how accurately can the initial velocity be inferred from a later one?

We study two generalized Genesis models and a power-law contracting stage.

Main distinction: attraction of the homogeneous background and stability of perturbations are separate properties.

Genesis and pre-bounce contraction

Genesis: expansion from an asymptotically Minkowski state,

$$a(t) \to a_{-\infty} > 0, \qquad H \to 0^{+}, \qquad t \to -\infty,$$

with $\dot{H} > 0$ during Genesis.

Power-law contraction:

$$a(t) = d(-t)^{\chi}, \qquad H = \frac{\chi}{t} < 0, \qquad t < 0, \quad 0 < \chi < 1.$$

The selected contracting model describes the stage **before** the bounce.

A common reduction for all three models

The models belong to the Horndeski subclass $G_4 = G_4(\phi)$, $G_5 = 0$.

$$\psi = e^{-\lambda\phi} > 0, \qquad v = \dot{\psi}, \qquad \dot{\phi} = -\frac{v}{\lambda\psi}.$$

The background equations take the form

$$\mathcal{E}(\psi, v, H) = 0, \qquad \mathcal{P} = P_0 + P_v\dot{v} + P_H\dot{H} = 0.$$

Differentiating the constraint and solving for the time derivatives gives

$$\dot{\psi} = v, \qquad \dot{v} = F_j(\psi, v).$$

In the sector $v < 0$, increasing cosmic time corresponds to decreasing ψ.

Two Hubble branches and their regular domain

$$AH^2 + BH + C = 0, \qquad H_\pm = \frac{-B \pm \sqrt{\mathcal{D}}}{2A}, \qquad \mathcal{D} = B^2 - 4AC.$$

For $\mathcal{D} > 0$, two distinct real Hubble roots define two reduced flows.

A regular branchwise evolution requires

$$v \neq 0, \qquad \mathcal{D} > 0, \qquad \Delta = \mathcal{E}_v P_H - \mathcal{E}_H P_v \neq 0,$$

with $G_4 \neq 0$ and smooth coefficients.

The labels $H_\pm$ do not determine expansion or contraction; the sign of H does.

Forward sensitivity and inverse reconstruction

Compare velocities at fixed field sections on a continuously followed branch:

$$\psi_i > \psi_f > 0, \qquad v_i \longmapsto v_f, \qquad J_j = \left.\frac{\partial v_f}{\partial v_i}\right|_{\psi_i,\psi_f,j}.$$

$$\delta v_f = J_j \delta v_i, \qquad \mathcal{A}_{\mathrm{inv},j} = \frac{1}{|J_j|}.$$

For $\mathrm{d}v/\mathrm{d}\psi = g_j(\psi, v)$, every finite regular segment gives

$$J_j = \exp\left[\int_{\psi_i}^{\psi_f} \partial_v g_j \,\mathrm{d}\psi\right] > 0.$$

A small J_j suppresses forward differences and amplifies inverse errors. The map remains locally invertible.

Genesis: the common scalar-field limit

Neglecting gravitational backreaction gives a first integral,

$$\hat{\rho}(Y) = C\psi^p, \qquad Y = \frac{v^2}{2\lambda^2}, \qquad p = 2(\alpha + 1).$$

Near any simple nonzero Genesis root, linearization yields

$$J^{\mathrm{asym,lin}} = \left(\frac{\psi_f}{\psi_i}\right)^p, \qquad \mathcal{A}_{\mathrm{inv}}^{\mathrm{asym,lin}} = \left(\frac{\psi_i}{\psi_f}\right)^p.$$

For $\alpha = 2.02$, $p = 6.04$; the section pair $(100, 50)$ gives 65.80.

This leading law applies to both healthy and unstable simple roots.

Model 1: one nontrivial Genesis solution

$$g_2 = -Y + Y^2, \qquad g_3 = Y, \qquad G_4 = \frac{M_{\rm Pl}^2}{2}, \qquad G_5 = 0.$$

$$q = 3 - 4\lambda(\alpha - 1) > 0, \qquad Y_0 = \frac{1}{q}, \qquad v_{\rm G} = -\lambda\sqrt{\frac{2}{q}}.$$

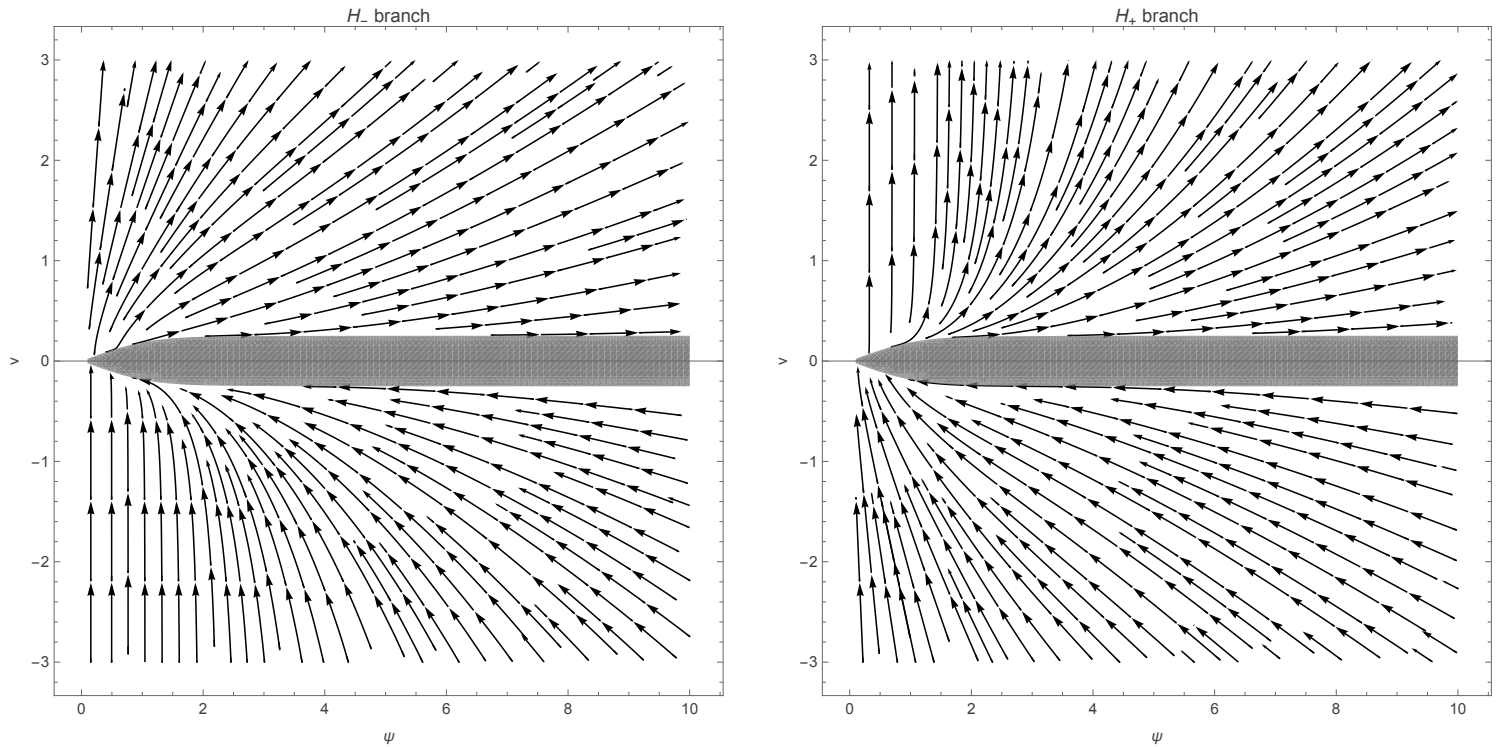
The benchmark is

$$\alpha = 2.02, \qquad \lambda = 0.25, \qquad M_{\rm Pl} = 1, \qquad v_{\rm G} \simeq -0.251.$$

It is stable at quadratic order in the asymptotic Genesis regime:

$$c_s^2 \simeq 0.515, \qquad c_T^2 = 1, \qquad n_s = 0.96.$$

Model 1: phase portraits on the two branches



H_- on the left, H_+ on the right; gray shading denotes $\mathcal{D} < 0$.

The expanding Genesis benchmark belongs to H_+ once the correction to v_{G} is included.

Model 1: gravity changes the sensitivity

Use the same benchmark and $v_i = v_{\mathrm{G}} - 10^{-4}$.

(ψ_i, ψ_f)	$\mathcal{A}_{\mathrm{inv},-}$	$\mathcal{A}_{\mathrm{inv},+}$	$\mathcal{A}_{\mathrm{inv},0}$
$(100, 50)$	69.24	62.45	65.80
$(100, 40)$	301.71	217.46	253.25
$(100, 30)$	4741.29	846.52	1439.42

$\mathcal{A}_{\mathrm{inv},0}$ is the **linearized scalar-field estimate**.

The full dynamics gives branch-dependent factors that can differ substantially from this estimate.

Model 2: two roots with different perturbative properties

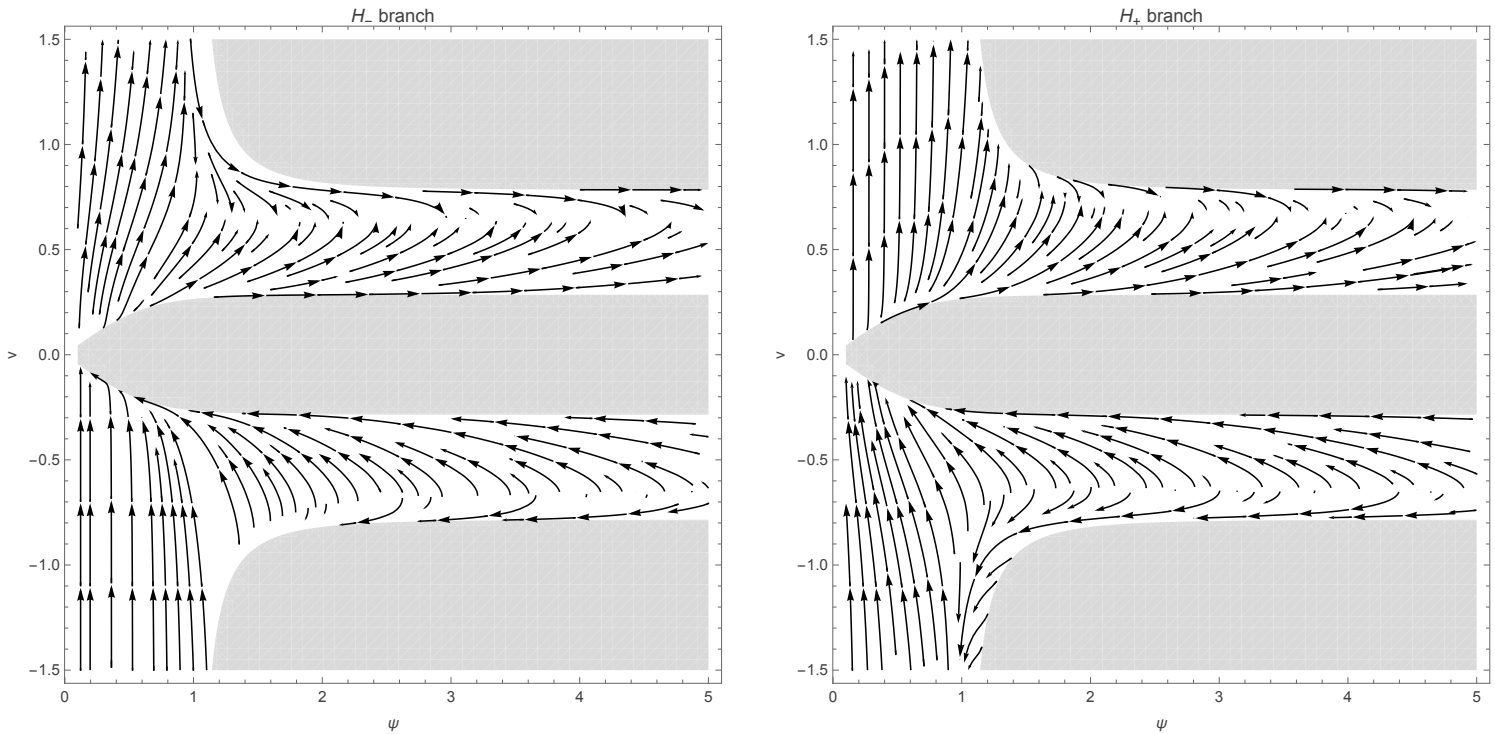
$$g_2 = -Y + 3Y^2 - Y^3, \qquad g_3 = Y, \qquad A_2 = 9 - 4\lambda(\alpha - 1),$$

$$Y_{0,\pm} = \frac{A_2 \pm \sqrt{A_2^2 - 20}}{10}, \qquad A_2 > 2\sqrt{5}.$$

For $\alpha = 2.02$, $\lambda = 0.5$, $M_{\rm Pl} = 1$:

	$Y_{0,-}$	$Y_{0,+}$
Y_0	0.1627	1.2293
$v_{\rm G}$	-0.2852	-0.7840
c_s^2	0.256	-0.656
Scalar sector	Healthy asymptotically	Ghost and gradient instabilities

Model 2: phase space with two Genesis roots



H_-

on the left, H_+ on the right; gray shading denotes $\mathcal{D} < 0$.

As $\psi \to \infty$: $v_{\mathrm{G},+} \leq v \leq v_{\mathrm{G},-}$. Both expanding benchmark asymptotics are associated with H_+.

Model 2: convergence near healthy and unstable roots

$$\psi_i = 100, \quad \psi_f = 50, \quad \alpha = 2.02, \quad \lambda = 0.5, \quad M_{\rm Pl} = 1,$$

$$v_i = v_{\rm G,-} - 10^{-4} \quad \text{or} \quad v_i = v_{\rm G,+} + 10^{-4}.$$

Selected root	$\mathcal{A}_{\rm inv,-}$	$\mathcal{A}_{\rm inv,+}$	$\mathcal{A}_{\rm inv}^{\rm asym,exact}$
$Y_{0,-}$: healthy	66.55	64.87	65.70
$Y_{0,+}$: unstable	77.39	57.35	65.88

The last column is the **exact nonlinear** scalar-field estimate at the same v_i.

Physical implication

Homogeneous velocity differences can decrease even near a background with ghost and gradient instabilities.

For these initial data, $H_+ < 0 < H_-$: the H_+ trajectories start in contraction.

Model 3: two contracting Hubble branches

The gravitational coupling depends on the scalar field:

$$G_4 = \frac{\hat{g}}{2} e^{2\mu\phi}, \qquad G_5 = 0, \qquad \psi = e^{-\phi}, \qquad d_3 = -2.$$

The constraint and its roots are

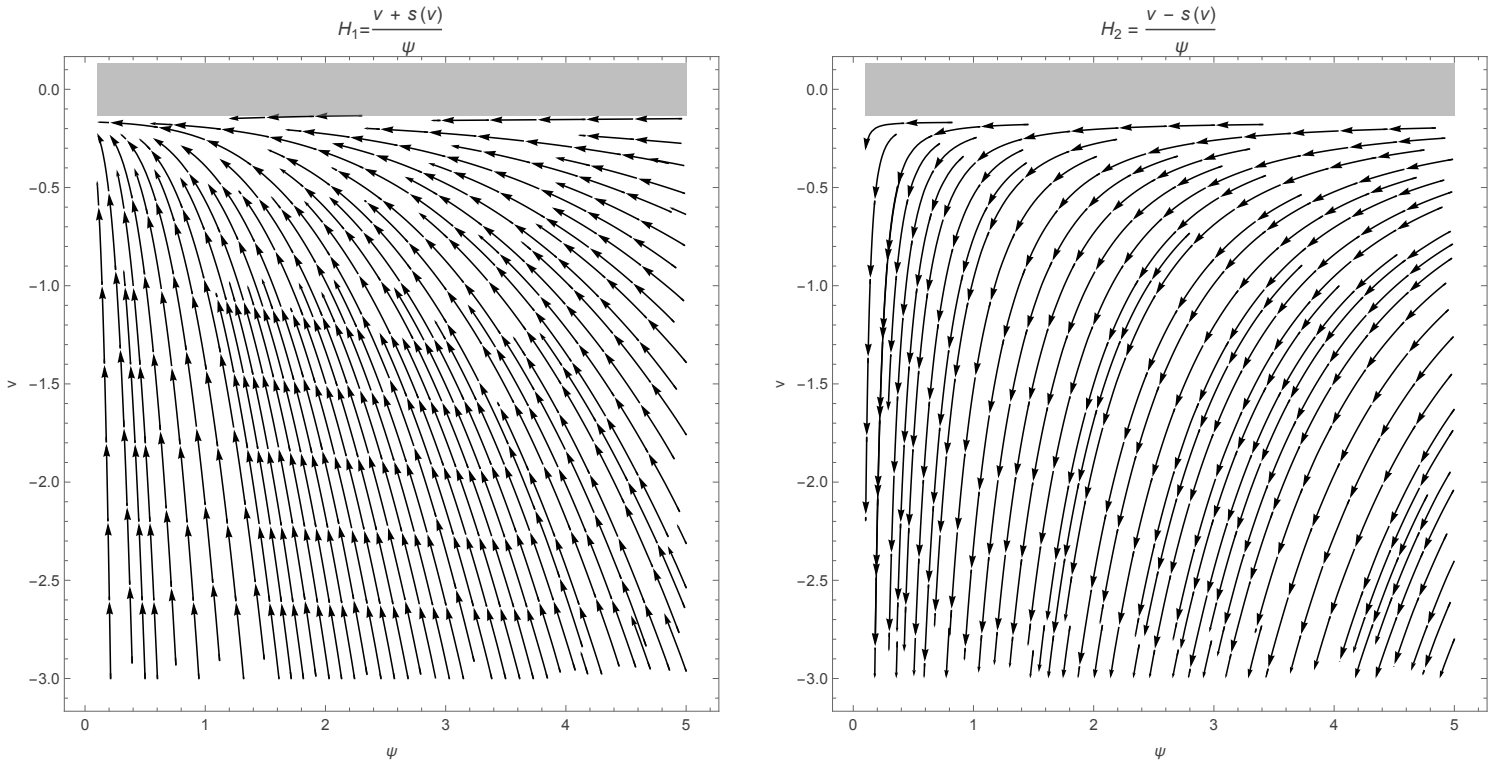
$$3\psi^2 H^2 - 6\psi v H + c_2 = 0,$$

$$H_1 = \frac{v + s(v)}{\psi}, \qquad H_2 = \frac{v - s(v)}{\psi}, \qquad s(v) = \sqrt{v^2 - c_2/3}.$$

The benchmark has $\mu = 1.0099$, $c_2 = 0.053$, $\kappa = 1$, $\hat{g} = 1$. For $v < -\sqrt{c_2/3}$, both branches contract.

For $c_2 > 0$, $H = 0$ is impossible in this stage: the bounce needs an interpolating Lagrangian.

Model 3: phase portraits during contraction



H_1 (left): attractor $v_*^{(1)} \simeq -0.166010$; H_2 (right): repeller $v_*^{(2)} \simeq -0.167338$.

Gray shading denotes $|v| < \sqrt{c_2/3}$; both panels show $v < 0$.

Model 3: the attraction exponent

For a constant-velocity power-law solution,

$$a = d(-t)^{\chi_j}, \qquad \delta v \propto \psi^{\gamma_j}, \qquad \gamma_j = 3(1-\chi_j) + 2(\mu - 1).$$

	H_1	H_2
χ_j	0.40087	1.60753
γ_j	1.81720	-1.80278
As ψ decreases	Attraction	Repulsion

H_1 belongs to the selected class $0 < \chi_1 < 1$; $\chi_2 > 1$ is outside it. The classification above refers to the stated benchmark.

Model 3: an exact sensitivity formula

The reduced flow is autonomous in $\ln\psi$:

$$\frac{\mathrm{d}v}{\mathrm{d}\ln\psi} = Q_j(v), \qquad Q_j(v) = \frac{F_j(v)}{v}, \qquad \dot{v} = \frac{F_j(v)}{\psi}.$$

On nonstationary regular trajectories with $Q_j \neq 0$,

$$J_j = \frac{Q_j(v_f)}{Q_j(v_i)}, \qquad \mathcal{A}_{\mathrm{inv},j} = \left|\frac{Q_j(v_i)}{Q_j(v_f)}\right|.$$

On the constant-velocity reference solution, the variational equation gives

$$J_j = \left(\frac{\psi_f}{\psi_i}\right)^{\gamma_j}, \qquad \mathcal{A}_{\mathrm{inv},j} = \left(\frac{\psi_i}{\psi_f}\right)^{\gamma_j}.$$

Model 3: finite-interval sensitivity

For $v_i^{(j)} = v_*^{(j)} - 10^{-4}$, the full reduced dynamics gives

(ψ_i, ψ_f)	$\mathcal{A}_{\mathrm{inv},1}$	$\mathcal{A}_{\mathrm{inv},2}$
$(100, 80)$	1.501	0.668
$(100, 50)$	3.529	0.285
$(100, 30)$	8.933	0.112

On the attracting branch H_1, inverse velocity errors are amplified.

On the repelling branch H_2, inverse velocity errors are suppressed.

For fixed initial velocity, the map depends only on the section ratio ψ_f/ψ_i.

Long-wavelength modes: from backgrounds to correlators

Spatial perturbations are Fourier modes, $\zeta(t,\mathrm{x}) = \int \frac{\mathrm{d}^3 k}{(2\pi)^3}\, \zeta_{\mathrm{k}}(t) e^{i\mathrm{k}\cdot\mathrm{x}}$.

$$S_\zeta^{(2)} = \int \mathrm{d}t\, \mathrm{d}^3x\, a^3 \mathcal{G}_S \left[\dot{\zeta}^2 - \frac{c_s^2}{a^2}(\partial_i \zeta)^2\right].$$

For negligible spatial gradients ($k \to 0$),

$$\frac{\mathrm{d}}{\mathrm{d}t}\left(a^3 \mathcal{G}_S \dot{\zeta}_k\right) \simeq 0 \quad \Longrightarrow \quad \boxed{\zeta_k \simeq C_{1,k} + C_{2,k} \int^t \frac{\mathrm{d}t'}{a^3 \mathcal{G}_S}.}$$

Cosmological collider: study the squeezed bispectrum, $k_L \ll k_S$, where a long mode is correlated with two short modes:

$$\langle \zeta_{\mathrm{k}_L} \zeta_{\mathrm{k}_S} \zeta_{-\mathrm{k}_L - \mathrm{k}_S} \rangle' = B_\zeta(k_L, k_S, |\mathrm{k}_L + \mathrm{k}_S|).$$

Caution: homogeneous δv and physical $\zeta_{k\to 0}$ are not the same perturbation.

Sources: Nishi–Kobayashi (2015), Sec. IV; Arkani-Hamed–Maldacena (2015).

Our models: background attraction vs. long modes

Generalized Genesis (Models 1 and 2, $\alpha = 2.02$):

$$\delta v \propto \psi^{2(\alpha+1)} \propto (-t)^{6.04},$$
$$\mathcal{G}_S \propto (-t)^{2\alpha}, \quad a \simeq 1 \quad \Longrightarrow \quad \zeta_k^{\rm nc} \propto (-t)^{1-2\alpha} = (-t)^{-3.04}.$$

For $\psi_f/\psi_i = 1/2$ (both sections in the asymptotic regime):

$$\boxed{\frac{\delta v_f}{\delta v_i} \simeq 2^{-6.04} = 0.0152, \qquad \frac{\zeta_{k,f}^{\rm nc}}{\zeta_{k,i}^{\rm nc}} \simeq 2^{3.04} = 8.22.}$$

Pre-bounce contraction (Model 3, physical branch H_1):

$$a \propto (-t)^{\chi}, \quad \mathcal{G}_S \propto (-t)^{-2\mu}, \quad \gamma_1 = 2\mu + 1 - 3\chi_1 \simeq 1.8172,$$

$$\boxed{\delta v \propto \psi^{\gamma_1}, \quad \zeta_k^{\rm nc} \propto (-t)^{\gamma_1}, \quad \left.\frac{\delta v_f}{\delta v_i}\right|_{\psi_f/\psi_i=1/2} \simeq 2^{-1.8172} = 0.284.}$$

Results are asymptotic, for the nonconstant long mode; for Model 2 use the healthy $Y_{0,-}$ root.

Sources: arXiv:2610.36036; Nishi–Kobayashi (2015).

A possible collider extension: massive field in Genesis

Add a *spectator* σ coupled to a conformal metric (not part of our original three Horndeski models):

$$\hat{g}_{\mu\nu} = e^{2\lambda\phi} g_{\mu\nu}, \qquad \hat{a} \simeq \frac{1}{H_{\rm eff}(-t)}, \qquad H_{\rm eff} = \lambda\sqrt{2Y_0}.$$

At $k|t| \ll 1$, a free massive mode has the indices

$$\sigma_k \propto (-t)^{\Delta_\pm}, \quad \Delta_\pm = \frac{3}{2} \pm i\nu, \qquad \nu = \sqrt{\frac{m_\sigma^2}{H_{\rm eff}^2} - \frac{9}{4}} \quad (m_\sigma > \tfrac{3}{2}H_{\rm eff}).$$

Healthy Genesis benchmarks (in the models' parameter units):

	Y_0	$H_{\rm eff}$	$m_{\rm threshold} = 3H_{\rm eff}/2$
Model 1	0.5051	0.2513	0.3769
Model 2 ($Y_{0,-}$)	0.1627	0.2852	0.4278

Next step: compute the mixing and cubic vertices transferring this massive-field signal to the squeezed ζ bispectrum. Check weak coupling and the exit/transition.

Sources: Nishi–Kobayashi (2015), Sec. V; Arkani-Hamed–Maldacena (2015). Illustrative linear indices; no bispectrum computed.

Strong convergence depends on the chosen variable

Under a regular change of variable $u = u(\psi, v)$,

$$J_u = \frac{u_v(\psi_f, v_f)}{u_v(\psi_i, v_i)} J_v.$$

For Model 1 on H_- between the sections $(100, 30)$,

$$J_v \simeq 2.109 \times 10^{-4}, \qquad \frac{\partial H_f}{\partial H_i} \simeq 0.99999.$$

Strong suppression in v therefore need not imply comparable suppression in H.

The factors depend on the variable, sections, and branch; they do not define an invariant loss of information.

Conclusions and scope

Genesis: gravitational backreaction changes finite-interval sensitivity and distinguishes the two Hubble branches.

Homogeneous attraction can coexist with unstable perturbations.

Power-law contraction: for the benchmark, H_1 attracts and H_2 repels; the sensitivity admits an exact expression.

Inverse reconstruction can be ill-conditioned while evolution remains locally unique.

Perturbative control must be checked independently. Transfer of deviations through the bounce remains an open calculation; collider signals require a separate correlation-function analysis.

Source: paper, Secs. 4–6.

The full Horndeski action

$$S = \int \mathrm{d}^4x\sqrt{-g}\sum_{i=2}^{5}\mathcal{L}_i, \qquad X = -\frac{1}{2}g^{\mu\nu}\partial_\mu\phi\partial_\nu\phi.$$

$$\begin{aligned}
\mathcal{L}_2 &= G_2(\phi, X),\\
\mathcal{L}_3 &= -G_3(\phi, X)\Box\phi,\\
\mathcal{L}_4 &= G_4 R + G_{4X}\left[(\Box\phi)^2 - (\nabla_\mu\nabla_\nu\phi)^2\right],\\
\mathcal{L}_5 &= G_5 G^{\mu\nu}\nabla_\mu\nabla_\nu\phi\\
&\quad - \frac{G_{5X}}{6}\left[(\Box\phi)^3 - 3\Box\phi(\nabla_\mu\nabla_\nu\phi)^2 + 2(\nabla_\mu\nabla_\nu\phi)^3\right].
\end{aligned}$$

$$(\nabla_\mu\nabla_\nu\phi)^2 = (\nabla_\mu\nabla_\nu\phi)(\nabla^\mu\nabla^\nu\phi),$$

$$(\nabla_\mu\nabla_\nu\phi)^3 = (\nabla_\mu\nabla_\nu\phi)(\nabla^\nu\nabla^\rho\phi)(\nabla_\rho\nabla^\mu\phi).$$

Metric signature: $(-,+,+,+)$; $R = 6(\dot{H} + 2H^2)$ on a spatially flat FLRW background.

Source: paper, Sec. 2.1; Horndeski, 1974; Kobayashi et al., 2011.

The Horndeski subclass shared by all three models

$$S = \int \mathrm{d}^4x\sqrt{-g}\left[G_2(\phi, X) - G_3(\phi, X)\Box\phi + G_4(\phi)R\right],$$

$$\mathrm{d}s^2 = -\mathrm{d}t^2 + a^2(t)\delta_{ij}\mathrm{d}x^i\mathrm{d}x^j, \quad \phi = \phi(t), \quad X = \dot{\phi}^2/2.$$

Independent background equations: $G_4 = G_4(\phi)$, $G_5 = 0$

$$\mathcal{E} = 2XG_{2X} - G_2 - 2XG_{3\phi} + 6H\dot{\phi}(XG_{3X} - G_{4\phi}) - 6H^2G_4 = 0,$$
$$\mathcal{P} = G_2 - 2X(G_{3\phi} + \ddot{\phi}G_{3X}) + 2(3H^2 + 2\dot{H})G_4 + 2(\ddot{\phi} + 2H\dot{\phi})G_{4\phi} + 4XG_{4\phi\phi} = 0.$$

Here $\mathcal{E}$ and $\mathcal{P}$ include the gravitational contributions.

Source: paper, Secs. 2.1 and 3.2; Kobayashi et al., 2011.

From the background equations to a linear system

After the field redefinition, $\mathcal{P} = 0$ is linear in $\dot{v}$ and $\dot{H}$:

$$\mathcal{P} = P_0 + P_v \dot{v} + P_H \dot{H} = 0, \quad P_v = \frac{2}{\lambda\psi}(X G_{3X} - G_{4\phi}), \quad P_H = 4 G_4.$$

The subscripts in P_v and P_H denote **coefficients**, not derivatives.

$$\frac{\mathrm{d}\mathcal{E}}{\mathrm{d}t} = \mathcal{E}_\psi v + \mathcal{E}_v \dot{v} + \mathcal{E}_H \dot{H} = 0.$$

Determining the time derivatives

$$\begin{pmatrix} \mathcal{E}_v & \mathcal{E}_H \\ P_v & P_H \end{pmatrix} \begin{pmatrix} \dot{v} \\ \dot{H} \end{pmatrix} = - \begin{pmatrix} \mathcal{E}_\psi v \\ P_0 \end{pmatrix}, \qquad \Delta = \mathcal{E}_v P_H - \mathcal{E}_H P_v.$$

Each partial derivative of $\mathcal{E}$ holds the other arguments fixed.

Source: paper, Sec. 3.3; the full expression for P_0 is given in the appendix.

Reduced flow on each branch

For $\Delta \neq 0$, Cramer's rule gives

$$\dot{v} = \frac{\mathcal{E}_H P_0 - \mathcal{E}_\psi v P_H}{\Delta}, \qquad \dot{H} = \frac{\mathcal{E}_\psi v P_v - \mathcal{E}_v P_0}{\Delta}.$$

Autonomous system in the phase plane

$$\dot{\psi} = v, \qquad \dot{v} = F_\pm(\psi, v),$$

$$F_\pm(\psi, v) = F(\psi, v, H_\pm(\psi, v)), \qquad F = \frac{\mathcal{E}_H P_0 - \mathcal{E}_\psi v P_H}{\Delta}.$$

$$H = H_\pm(\psi, v), \qquad \dot{a} = a H_\pm(\psi, v).$$

Regular domain: $G_4 \neq 0$, $\mathcal{D} > 0$, $\Delta \neq 0$, with smooth coefficients.

Source: paper, Sec. 3.3.

Three exceptional sets with distinct meanings

$\mathcal{D} = 0$: the roots $H_\pm$ coalesce; $\mathcal{E}_H = \pm\sqrt{\mathcal{D}} = 0$. The representation of the constraint by two graphs $H_\pm(\psi, v)$ breaks down.

$v = 0$: a scalar turning point; replacing the scalar equation with $\dot{\mathcal{E}} = 0$ loses independent information.

$\Delta = 0$, $v \neq 0$: a singular evolution matrix; on a regular real branch this corresponds to a vanishing scalar kinetic coefficient.

Identity on the constraint in this subclass

$$\mathcal{G}_S \mathcal{D} = 18 G_4 v \Delta.$$

For $v \neq 0$, $\mathcal{D} > 0$, $G_4 \neq 0$: $\quad \Delta = 0 \iff \mathcal{G}_S = 0$.

None of these conditions alone implies a curvature singularity.

Source: paper, Sec. 3.3.

The coefficient P_0 and determinant factorization

$$U = \frac{v^2}{\lambda\psi^2}, \quad W = \frac{1}{\lambda\psi}, \quad K = XG_{3X} - G_{4\phi}, \qquad \ddot{\phi} = U - W\dot{v}.$$

$$P_0 = G_2 - 2X(G_{3\phi} + UG_{3X}) + 6H^2 G_4 + 2(U + 2H\dot{\phi})G_{4\phi} + 4XG_{4\phi\phi}.$$

$$P_v = 2WK, \quad P_H = 4G_4, \qquad \Delta = \frac{4v}{\lambda^2\psi^2}\mathcal{K}_{\rm red},$$

$$\mathcal{K}_{\rm red} = G_4\big[G_{2X} + 2XG_{2XX} - 2G_{3\phi} - 2XG_{3\phi X} + 6H\dot{\phi}(G_{3X} + XG_{3XX})\big] + 3(XG_{3X} - G_{4\phi})^2.$$

Why $v = 0$ requires the original scalar equation

$$\dot{\mathcal{E}} + 3H(\mathcal{E} + \mathcal{P}) = \dot{\phi}\,\mathcal{C}_\phi.$$

At $\dot{\phi} = 0$, the identity does not imply $\mathcal{C}_\phi = 0$ from the metric equations.

Source: paper, Sec. 3.3.

Generalized Genesis: the common family of both examples

$$G_2 = e^{2(\alpha+1)\lambda\phi} g_2(Y), \quad G_3 = e^{2\alpha\lambda\phi} g_3(Y), \quad G_4 = \frac{M_{\rm Pl}^2}{2}, \quad G_5 = 0,$$

$$Y = e^{-2\lambda\phi} X = \frac{\nu^2}{2\lambda^2}, \qquad \alpha > 0, \quad \lambda > 0.$$

$$\hat{\rho}(Y) = 2Yg_2' - g_2 - 4\lambda Y(\alpha g_3 - Yg_3'),$$
$$\hat{p}(Y) = g_2 - 4\alpha\lambda Y g_3, \qquad \mathcal{G}(Y) = M_{\rm Pl}^2.$$

Asymptotic solution: $\hat{\rho}(Y_0) = 0,\ Y_0 > 0,\ \hat{p}(Y_0) < 0$

$$e^{\lambda\phi} \simeq \frac{1}{\lambda\sqrt{2Y_0}(-t)}, \quad H \simeq \frac{h_0}{(-t)^{2\alpha+1}}, \quad a \simeq 1 + \frac{h_0}{2\alpha(-t)^{2\alpha}}, \quad h_0 > 0.$$

This is the early-time asymptotic regime $t \to -\infty$, $H|t| \ll 1$.

Source: paper, Sec. 4.1; Nishi, Kobayashi, 2015.

Discriminants of the Genesis models

Model 1, $q = 3 - 4\lambda(\alpha - 1)$:

$$\mathcal{D}_1 = \frac{3v^2}{\lambda^6 \psi^{2+4\alpha}} \left[3v^4 + M_{\rm Pl}^2 \lambda^2 \psi^{2\alpha}(qv^2 - 2\lambda^2)\right], \quad \mathcal{D}_{1,\rm G} = \frac{72}{q^3 \psi^{2+4\alpha}}.$$

Model 2, $A_2 = 9 - 4\lambda(\alpha - 1)$:

$$\mathcal{D}_2 = \frac{3v^2}{2\lambda^6 \psi^{2+4\alpha}} \left[6v^4 + M_{\rm Pl}^2 \psi^{2\alpha} \left(2A_2 \lambda^2 v^2 - 5v^4 - 4\lambda^4\right)\right],$$

$$\mathcal{D}_{2,\rm G,\pm} = \frac{72 Y_{0,\pm}^3}{\psi^{2+4\alpha}} > 0.$$

Geometry of the allowed region in Model 2

The expression in square brackets equals

$$6v^4 - 5M_{\rm Pl}^2 \psi^{2\alpha}(v^2 - v_{\rm G,-}^2)(v^2 - v_{\rm G,+}^2).$$

Values on the Genesis lines refer to the leading asymptotic velocities.

Source: paper, Secs. 4.1–4.2.

Genesis: stability regions and the nonlinear scalar-field solution

Model 1: $q > 0$, $4\alpha\lambda > 1$; for $\alpha > 1$:

$$\frac{1}{4\alpha} < \lambda < \frac{3}{4(\alpha - 1)}.$$

Requiring $c_s^2 \leq 1$ for $\alpha > 1/2$ also gives $\lambda \leq 1/(2\alpha - 1)$. For $\alpha = 2.02$: $0.1238 < \lambda < 0.7353$; imposing $c_s^2 \leq 1$ gives $\lambda \leq 0.3289$.

Model 2, healthy root $Y_{0,-}$:

$$\lambda > \lambda_{\rm stab}(\alpha) = \frac{3(\alpha + 1) + \sqrt{24\alpha^2 + 28\alpha + 9}}{4\alpha(3\alpha + 2)}.$$

For $\alpha > 1$, also require $\lambda < (9 - 2\sqrt{5})/[4(\alpha - 1)]$. For $\alpha = 2.02$: $\lambda_{\rm stab} \simeq 0.3355$, with an upper bound of 1.1098.

Model 1: exact solution within the scalar-field approximation

$$Y_f = \frac{1 + \sqrt{1 + 4q\hat{\rho}(Y_i)(\psi_f/\psi_i)^p}}{2q}, \qquad v_f = -\lambda\sqrt{2Y_f}, \quad Y_i, Y_f > \frac{1}{2q}.$$

Source: paper, Secs. 4.1–4.2 and 5.1.

Genesis spectra and the limits of quadratic stability

$$n_s = \begin{cases} 3 + 2\alpha, & 0 < \alpha < 1/2, \\ 5 - 2\alpha, & \alpha > 1/2. \end{cases}$$

For $\alpha > 1/2$: $\zeta_k \propto (-t)^{1-2\alpha}$. The final spectrum inherits this tilt if the growing mode is transferred with a nonzero, nearly k-independent coefficient and dominates after the transition.

$$S_h^{(2)} = \frac{M_{\rm Pl}^2}{8} \int \mathrm{d}t\, \mathrm{d}^3x\, a^3 \left[\dot{h}_{ij}^2 - \frac{1}{a^2} (\partial_k h_{ij})^2 \right].$$

$c_T^2 = 1$; the tensor sector is free from ghosts and gradient instabilities.

For $a \simeq 1$ in the leading asymptotic regime, tensor vacuum modes are not amplified.

Final amplitudes and tensor production at exit require a transition analysis.

For $\alpha \simeq 2$, cubic interactions limit perturbative control.

Source: paper, Secs. 4.1–4.2; Nishi, Kobayashi, 2015; Akama, Hirano, 2023.

Genesis with gravitational backreaction

$$g_{\pm}(\psi, v) = \frac{F(\psi, v, H_{\pm}(\psi, v))}{v}, \qquad \frac{\mathrm{d}J_{\pm}}{\mathrm{d}\psi} = \partial_v g_{\pm} J_{\pm}.$$

The derivative includes the dependence of the selected Hubble root H

$$\partial_v g_{\pm} = \frac{F_v + F_H H_{\pm,v}}{v} - \frac{F}{v^2}, \qquad H_{\pm,v} = -\frac{\mathcal{E}_v}{\mathcal{E}_H}.$$

The partial derivative F_v holds ψ and H fixed.

Integrate the trajectory together with the variational equation.

Finite differences of nearby trajectories provide a convergence check.

Monitor the Friedmann constraint, the selected branch, and regularity.

Source: paper, Sec. 5.1, including the methodological clarification in the footnote.

Model 1: gravity modifies the finite-interval sensitivity

$$\alpha = 2.02, \quad \lambda = 0.25, \quad M_{\mathrm{Pl}} = 1, \quad v_i = v_{\mathrm{G}} - 10^{-4}.$$

(ψ_i, ψ_f)	$\mathcal{A}_{\mathrm{inv},-}$	$\mathcal{A}_{\mathrm{inv},+}$	$\mathcal{A}_{\mathrm{inv},0}$
$(100, 50)$	69.24	62.45	65.80
$(100, 40)$	301.71	217.46	253.25
$(100, 30)$	4741.29	846.52	1439.42
$(10, 8)$	5.69	2.90	3.85
$(10, 7.5)$	11.56	3.76	5.68
$(10, 7)$	40.17	4.82	8.62
$(10, 6.9)$	65.44	5.06	9.40
$(10, 6.8)$	154.89	5.30	10.27

$\mathcal{A}_{\mathrm{inv},0} = (\psi_i/\psi_f)^{6.04}$ is the **linearized** scalar-field estimate. The subscript 0 denotes neither a Friedmann branch nor the condition $H = 0$.

Source: paper, Sec. 5.1; the numerical table is reproduced in full.

Model 3: reduced equations of motion

In the open sector $v < -\sqrt{c_2/3}$, define

$$\kappa = c_3(1+2\mu) - d_2, \qquad s(v) = \sqrt{v^2 - c_2/3}.$$

Evolution on the two branches

$$\dot{\psi} = v,$$

$$\dot{v}_1 = -\frac{s(v)}{2\psi}\big[\kappa + 6v - 4(\mu-1)s(v)\big],$$

$$\dot{v}_2 = \frac{s(v)}{2\psi}\big[\kappa + 6v + 4(\mu-1)s(v)\big].$$

$\hat{g} = 1, \quad \mu = 1.0099, \quad c_2 = 0.053, \quad c_3 = -5, \quad d_3 = -2, \quad d_2 = -16.099.$
These give $\kappa = 1$, $\varrho = c_2/\kappa^2 = 0.053 < 2/27$, and $v_{\mathrm{crit}} \simeq -0.132916$.

Source: paper, Sec. 4.3; equations apply in the sector $v < 0$.

Covariant functions of Model 3

$$G_2 = \hat{g} e^{2\mu\phi}\Big\{ e^{\phi}\left[c_2 e^{\phi} + \sqrt{2}(d_2 - c_3 - 2\mu c_3)\sqrt{X}\right] + 2\mu(d_3 + 2\mu) X \ln X \Big\},$$

$$G_3 = \frac{\hat{g}}{2} e^{2\mu\phi}(d_3 + 2\mu)(2 + \ln X),$$

$$G_4 = \frac{\hat{g}}{2} e^{2\mu\phi}, \qquad G_5 = 0.$$

Domain: $X > 0$, $\hat{g} > 0$. The logarithmic terms cancel in the background equations.

Evolution equation for $d_3 = -2$, $v < 0$

$$c_2 + 3\psi^2 H^2 + 2\psi^2 \dot{H} + \kappa v + 2(1 + 2\mu)v^2 - 2\psi\dot{v} - 4\mu\psi v H = 0.$$

The sign of the $\sqrt{X}$ term depends on the sector: here $\sqrt{2}e^{\phi}\sqrt{X} = -v/\psi^2$.

Source: paper, Sec. 4.3; Ageeva, Petrov, Rubakov, 2023, Appendix D.

Model 3: full evolution versus the linearized estimate

$$v_i^{(j)} = v_*^{(j)} - 10^{-4}, \qquad \gamma_1 \simeq 1.8172, \quad \gamma_2 \simeq -1.8028.$$

(ψ_i, ψ_f)	$\mathcal{A}_{\mathrm{inv},1}$	$\mathcal{A}_{\mathrm{inv},2}$	$\mathcal{A}^{\mathrm{lin}}_{\mathrm{inv},1}$	$\mathcal{A}^{\mathrm{lin}}_{\mathrm{inv},2}$
$(100, 80)$	1.501	0.668	1.500	0.669
$(100, 70)$	1.914	0.525	1.912	0.526
$(100, 50)$	3.529	0.285	3.524	0.287
$(100, 40)$	5.295	0.190	5.286	0.192
$(100, 30)$	8.933	0.112	8.916	0.114
$(10, 8)$	1.501	0.668	1.500	0.669
$(10, 5)$	3.529	0.285	3.524	0.287

H_1: inverse errors are amplified; H_2: inverse errors are suppressed. Equal factors at the same section ratio follow from autonomy.

Source: paper, Sec. 5.3; the numerical table is reproduced in full.

Model 3: perturbations on the selected power-law background

$$\mathcal{F}_S = \frac{\hat{g}}{2}\psi^{-2\mu} f_S, \quad \mathcal{G}_S = \frac{\hat{g}}{2}\psi^{-2\mu} g_S, \quad f_S = \frac{4(\mu-1)}{1-\chi}, \quad g_S = \frac{6}{(1-\chi)^2}.$$

$$c_s^2 = \frac{2}{3}(\mu-1)(1-\chi) \simeq 0.00395, \qquad \mathcal{G}_T = \mathcal{F}_T = \hat{g}\psi^{-2\mu} > 0, \quad c_T^2 = 1.$$

$$n_s - 1 = n_T = \frac{2(1-\mu)}{1-\chi}, \qquad n_s \simeq 0.96,$$

$$r = 8 g_S (c_s^2)^\nu \simeq 0.03035, \qquad \nu = \frac{1+2\mu-3\chi}{2(1-\chi)}.$$

Strong coupling when extrapolated to the infinite past

$$\frac{E_{\mathrm{strong},T}}{E_{\mathrm{class}}} \propto (-t)^{1-\mu} \longrightarrow 0 \quad (t \to -\infty,\ \mu > 1).$$

A finite controlled interval or a modification of the early evolution is required.

Source: paper, Sec. 4.3; values refer to $\chi = \chi_1$.

Power-law contraction: discriminant and decay exponent

$$c_2 = \frac{3\chi(2-\chi)}{N^2}, \qquad N = \frac{2}{\kappa}\left[1 + 2\mu - 2(\mu-1)\chi\right].$$

$$\mathcal{D}_{\mathrm{pl}} = \frac{36\hat{g}^2(1-\chi)^2}{N^2\psi^{2+4\mu}} = \frac{9\hat{g}^2\kappa^2(1-\chi)^2}{[1+2\mu-2(\mu-1)\chi]^2\psi^{2+4\mu}} > 0.$$

For $\mu > 1$, $\kappa > 0$, $0 < \chi < 1$, the discriminant imposes no additional restriction on the power-law background.

Agreement of the exponents

$$\gamma = 3(1-\chi) + 2(\mu-1) = 2\mu + 1 - 3\chi.$$

The nonconstant long-wavelength mode $\propto (-t)^{2\mu+1-3\chi}$ decays for $\gamma > 0$.

The positive-friction condition $2\mu - 3\chi > 0$ differs from the decay condition. Decay of small modes and anisotropies does not establish general nonlinear BKL stability.

Source: paper, Secs. 4.3 and 5.1.

Model 3: non-Gaussianity estimates

$$f_{\rm NL}^{\rm local} \simeq \frac{5(\mu-1)}{6(\mu-\chi)},$$
$$f_{\rm NL}^{\rm equil} \simeq \frac{85}{324} - \frac{5}{81 c_s^2},$$
$$f_{\rm NL}^{\rm enfold} \simeq \frac{1}{32}\left(1 - \frac{1}{c_s^2}\right).$$

Benchmark in the paper

$$f_{\rm NL}^{\rm local} \simeq 0.014, \qquad f_{\rm NL}^{\rm equil} \simeq -15.35, \qquad f_{\rm NL}^{\rm enfold} \simeq -7.87.$$

These are the first nonvanishing terms in an expansion in slowly varying parameters in the Einstein frame.

The observational comparison is given by Ageeva, Kotenko, Petrov (2025).

Source: paper, Sec. 4.3; Ageeva, Kotenko, Petrov, arXiv:2410.10742.

Key references

Y. A. Ageeva, A. K. Sharofeev. *Attractors and initial-condition sensitivity in Horndeski cosmologies.* arXiv:2610.36036

G. W. Horndeski. *Second-order scalar-tensor field equations in a four-dimensional space.* Int. J. Theor. Phys. **10** (1974) 363.

T. Kobayashi, M. Yamaguchi, J. Yokoyama. *Generalized G-inflation.* Prog. Theor. Phys. **126** (2011) 511. arXiv:1105.5723.

S. Nishi, T. Kobayashi. *Generalized Galilean Genesis.* JCAP **03** (2015) 057. arXiv:1501.02553.

References on contraction and perturbative control

Y. Ageeva, P. Petrov, V. Rubakov. *Generating cosmological perturbations in non-singular Horndeski cosmologies.* JHEP **01** (2023) 026. arXiv:2207.04071.

S. Akama, S. Hirano. *Primordial non-Gaussianity from Galilean Genesis without strong coupling problem.* Phys. Rev. D **107** (2023) 063504. arXiv:2211.00388.

Y. Ageeva, M. Kotenko, P. Petrov. *Primordial non-Gaussianities for nonsingular Horndeski cosmologies.* Phys. Rev. D **112** (2025) 063526. arXiv:2410.10742.

Bibliographic details are taken from the manuscript project's reference database. All main numerical results in this presentation are taken from the supplied source.